Size-sensitive melting characteristics of gallium clusters: Comparison of experiment and theory for Ga_{17}^+ and Ga_{20}^+

Sailaja Krishnamurty, S. Chacko, and D. G. Kanhere
Department of Physics, and Centre for Modeling and Simulation, University of Pune, Ganeshkhind, Pune-411 007, India

G. A. Breaux, C. M. Neal, and M. F. Jarrold
Chemistry Department, Indiana University, 800 East Kirkwood Avenue, Bloomington, Indiana 47405-7102, USA
(Received 21 July 2005; revised manuscript received 27 October 2005; published 9 January 2006)

Experiments and simulations have been performed to examine the finite-temperature behavior of Ga_{17}^+ and Ga_{20}^+ clusters. Specific heats and average collision cross sections have been measured as a function of temperature, and the results compared to simulations performed using first-principles density functional molecular dynamics. The experimental results show that while Ga_{17}^+ apparently undergoes a solid-liquid transition without a significant peak in the specific heat, Ga_{20}^+ melts with a relatively sharp peak. Our analysis of the computational results indicate a strong correlation between the ground-state geometry and the finite temperature behavior of the cluster. If the ground-state geometry is symmetric and "ordered" the cluster is found to have a distinct peak in the specific heat. However, if the ground-state geometry is amorphous or "disordered" the cluster melts without a peak in the specific heat.

DOI: 10.1103/PhysRevB.73.045406 PACS number(s): 61.46.−w, 36.40.Cg, 36.40.Ei

I. INTRODUCTION

It is now well established that the melting temperatures of particles with thousands of atoms decrease smoothly with decreasing particle size, due to the increase in the surface to volume ratio.[1,2] However, unlike particles with thousands of atoms or the bulk material, probing the finite temperature properties of small clusters (with <500 atoms) is nontrivial and remains a challenging task. Experimental studies of the melting transitions of clusters in the small size regime have only recently become possible.[3–11] Several interesting phenomena have been observed, including melting temperatures that rise above the bulk value[7,8] and strong size-dependent variations in the melting temperatures.[9,10] These experimental findings have motivated many theoretical investigations of the finite temperature behavior of clusters.[12–18] Simulations based on first principles have been particularly successful in quantitatively explaining the factors behind the size dependent variations in the melting behavior of clusters.[17] Thus, a confluence of recent advances in experimental methods and theoretical studies using first-principles methods have set the stage for a major increase in our understanding of phase transitions in these small systems.

Gallium clusters not only melt at substantially higher temperatures than the bulk ($T_{m[\mathrm{bulk}]}=303$ K),[8] but they also exhibit wide variations in the temperature dependencies of their specific heats, with some clusters showing strong peaks (due to the latent heat), while others (apparent "nonmelters") showing no peak.[9] These features show a strong dependence on the cluster size, where the addition of a single atom can change a cluster with no peak in the specific heat into a "magic melter" with a very distinct peak. This behavior has been observed for gallium clusters Ga_n, with $n=30-55$.

In the present work we probe the melting behavior of small gallium cluster ions and show that the "nonmelting" and "melting" features in the specific heats are observed in clusters as small as Ga_{17}^+ and Ga_{20}^+, respectively. Recently reported experimental results for Ga_{17}^+ show no evidence for a melting transition.[8] The experimental results in this case were specific heat measurements performed using multicollision induced dissociation, where a peak in the specific heat due to the latent heat was the signature of melting. On the other hand, recent simulations for Ga_{17} show a broad peak in the specific heat centered around 600 K. The previous specific heat measurements for Ga_{17}^+ only extended up to 700 K, so one possible explanation for this apparent discrepancy is that the melting transition occurred at a slightly higher temperature than examined in the experiments. Here, we report specific heat measurements for Ga_{17}^+ over a more extended temperature range along with specific heat measurements for Ga_{20}^+. While no peak is observed in the heat capacities for Ga_{17}^+, a peak is observed for Ga_{20}^+.

To further probe the melting transitions in these clusters, ion mobility measurements have been performed for Ga_{17}^+ and Ga_{20}^+ as a function of temperature. The ion mobility measurements provide average collision cross sections which can reveal information about the shape and volume changes that occur on melting. For example, a cluster with a nonspherical geometry might be expected to adopt a more spherical shape (a liquid droplet) on melting. If there is not a significant shape change, there may still be a volume change on melting. Most bulk materials expand when they melt (the liquid is less dense than the solid). Even in the absence of a significant shape or volume change, the cross sections might show an inflection at the melting transition due to the thermal coefficient of expansion of the liquid cluster being larger than for the solid (in the macroscopic regime most liquids have larger coefficients of expansion than the corresponding solids). An inflection is observed in the cross sections for both Ga_{17}^+ and Ga_{20}^+. Thus, the ion mobility measurements are consistent with the view that both Ga_{17}^+ and Ga_{20}^+ are in a liquidlike state above 800 K.

To explore the reasons behind the behavior outlined above (i.e., to determine why Ga_{17}^+ seems to melt without a peak in its specific heat, while a peak is observed for Ga_{20}^+), we have carried out first-principles density functional (DF) molecular dynamics (MD) calculations on the above clusters. We also examine and analyze the lowest energy geometries and nature of bonding in these clusters. The ionic specific heat is computed using multiple histogram method.[19,20] The calculated specific heat for Ga_{17}^+ shows three broad low intensity maxima that extend from 300 to 1400 K. This resembles the experimental result where the measured specific heat is relatively featureless. In contrast, the calculated specific heat for Ga_{20}^+ shows a clear peak around 750 K. This is in excellent agreement with the peak obtained from experimental measurements (which occurs at around 700 K). Finally, our theoretical results show that the features in the specific heat curves are influenced by the ground state geometry, the bonding of the atoms within the ground state structure, and the isomer distribution that is accessible as the temperature is increased.

In Sec. II, we present the experimental methods and the computational details. In Sec. III we discuss the experimental and theoretical results on Ga_{17}^+ and Ga_{20}^+. We conclude our results in Sec. IV.

II. METHODOLOGY

Specific heats were measured using the recently developed multi-collision induced dissociation approach. The cluster ions are generated by laser vaporization of a liquid gallium target in a continuous flow of helium buffer gas. After exiting the laser vaporization region of the source, the clusters travel through a 10 cm long temperature variable extension where their temperature is set. Cluster ions that exit the extension are focused into a quadrupole mass spectrometer where a particular cluster size is selected. The size selected clusters are then focused into a collision cell containing 1 Torr of helium. As the clusters enter the collision cell they undergo numerous collisions with the helium, each one converting a small fraction of the ions translational energy into internal energy. If the initial kinetic energy is high enough some of the cluster ions may be heated to the point where they dissociate. The dissociated and undissociated cluster ions are swept across the collision cell by a small electric field and some of them exit through a small aperture. The ions that exit are analyzed in a second quadrupole mass spectrometer and then detected by an off axis collision dynode and dual microchannel plates. The fraction of the ions that dissociate is determined from the mass spectrum. Measurements are performed as a function of the ions initial kinetic energy, and the initial kinetic energy required for 50% dissociation (IKE50%D) is determined from a linear regression. IKE50%D is measured as a function of the temperature of the source extension. IKE50%D decreases as the temperature is raised because hotter clusters have more internal energy, and hence less energy needs to be added in order to cause dissociation. At the melting transition a sharp decrease in IKE50%D is expected due to the latent heat. The derivative of IKE50%D with respect to temperature is approximately proportional to the specific heat. The proportionality constant is the fraction of the clusters initial kinetic energy that is converted into internal energy, which is estimated from an impulsive collision model. A drop in the IKE50%D values due to the latent heat of a melting transition leads to a peak in the specific heat.

Ion mobility measurements can provide information on the shape and volume changes that occur when clusters melt. For the ion mobility measurements, the collision cell is replaced by a 7.6 cm long drift tube. 50 μs pulses of cluster ions are injected into the drift tube and the drift time distribution is obtained by recording the ions arrival times at the detector with a multichannel scalar. Average collision cross sections are obtained from the drift time distributions using standard methods.[21,22]

All the simulations have been performed using Born Oppenheimer molecular dynamics based on Kohn-Sham formulation of density functional theory (DFT).[23] We have used Vanderbilt's ultrasoft pseudopotentials[24] within the generalized gradient approximation (GGA), as implemented in the VASP package.[25] For all the calculations, we take the $4s^2$ and $4p^1$ electrons as valence electrons and the $3d$ electrons[26] as a part of the ionic core. An energy cutoff of about 10 Ry is used for the plane wave expansion of the wavefunction, with a convergence in the total energy of the order of 0.0001 eV. Cubic supercells of lengths 20 and 25 Å are used for Ga_{17}^+ and Ga_{20}^+ respectively. The ionic phase space of the clusters is sampled by isokinetic MD where kinetic energy is held constant via a velocity scaling method. In order to have a reliable sampling, we split the total temperature range from 100–1400 K into 15 different temperatures. We maintain the cluster at each temperature for a period of at least 90 ps, leading to a total simulation time of around 1 ns. The resulting trajectory data was used to compute standard thermodynamic indicators as well as the ionic specific heat, via a multihistogram technique. The details can be found in Refs. 20 and 27.

III. RESULTS AND DISCUSSION

Specific heats measured for Ga_{17}^+ and Ga_{20}^+ as a function of temperature are shown in the lower half of Fig. 1. The points are the experimental values, while the dashed line is the prediction of a modified Debye model. In the case of Ga_{17}^+, the specific heats shown in Fig. 1 appear to gradually increase up to around 900 K. The sharp decrease in the specific heats above 900 K is an artifact due to evaporative cooling, the spontaneous unimolecular dissociation of the cluster ions as they travel between the source extension and the collision cell. For Ga_{20}^+, the specific heats show a broad maximum, around 400 K wide, centered at around 725 K. The peak for Ga_{20}^+ is significantly broader than observed for larger clusters (such as Ga_{39}^+ and Ga_{40}^+) where the peak was attributed to a melting transition. However, it is well known that the melting transition, and the corresponding peak in the specific heats, becomes broader with decreasing cluster size. Thus, even though the peak in the specific heats for Ga_{20}^+ is around 400 K wide, it is appropriate to assign it to a finite size analog of a bulk melting transition. The center of the peak is

FIG. 1. Color online Specific heats and average collision cross sections measured for size selected Ga_{17}^+ and Ga_{20}^+ clusters as a function of temperature. The solid blue points show the specific heats which are normalized to $3Nk_B$ the classical value , where k_B is the Boltzmann constant and $N= 3n-6+3/2 /3$ $n=$number of atoms in the cluster, and $3n-6$ and $3/2$ are due to the vibrational and rotational contributions, respectively . Error bars show the average uncertainties one standard deviation in the specific heats. The uncertainties in the cross sections are smaller than the points.

at around 725 K, this is well above the bulk melting point 303 K . This continues a trend reported for larger cluster sizes $n=30-55$ where the melting temperatures are also significantly above the bulk value. The unfilled red circles in Fig. 1 show the average collision cross sections determined for Ga_{17}^+ and Ga_{20}^+ as a function of the temperature. The cross sections are expected to systematically decrease with increasing temperature because the long range attractive interactions between the cluster ion and the buffer gas atoms becomes less important, and the collisions become harder as the temperature is raised.[21,22] The thick dashed red line in the figures show the expected exponential decrease in the cross sections with increasing temperature. There is an inflection in the cross sections for Ga_{20}^+ that appears to slightly precede the peak in the specific heat for this cluster. The inflection in consistent with a melting transition where the liquid cluster has a larger coefficient of thermal expansion than the solid. There is also a small inflection in the cross sections for Ga_{17}^+. We take this as evidence that a solid-liquid transition also occurs for Ga_{17}^+, but without a significant peak in the specific heat. The only other explanation for the absence of a peak in the specific heat for Ga_{17}^+ is that the melting transition occurs above 900 K or below 100 K.

To understand the reason behind different melting behavior of Ga_{17}^+ and Ga_{20}^+, we have carried out a detailed analysis of structure and bonding in both clusters. It turns out that the nature of the ground-state geometry and bonding plays a crucial role in determining their finite temperature behavior. We begin with a discussion of the equilibrium geometries of cationic Ga_{17} and Ga_{20} clusters. Roughly 500 initial configurations were selected and quenched using a quasi-Newton algorithm incorporated in VASP. These initial configurations were chosen from a high-temperature runs carried out above the melting temperature 900, 1000, 1200, and 1400 K, respectively , b from various geometries known in the literature,[12] and c by building the structures from Ga_{13} and Ga_{15}. The initial geometries yielded roughly 200 distinct equilibrium configurations for each cluster, which span an energy range of about 2.5 eV above the ground state. Thus, the sample of configurations is believed to be adequate. In Fig. 2 we show the lowest-energy structure along with some low lying geometries of both the clusters. The lowest-energy geometry of the Ga_{17}^+ cluster see Fig. 2 a 1 is similar to that of Ga_{17} reported in our earlier work.[12] It has a distorted decahedral structure distorted C_2 symmetry , which suggests the possibility of further cluster growth to a 19 atom double decahedron. In contrast, the ground-state geometry of Ga_{20}^+, shown in Fig. 2 b 1, is more symmetric C_{2v} . It can be described as a double decahedral structure of 19 atoms, where the atom capping the bottom merges into the pentagonal plane to form a hexagonal ring. In addition, an atom from

FIG. 2. The ground state and some representative low lying and excited state geometries of Ga_{17}^+ and Ga_{20}^+ clusters. Structure 1 corresponds to the ground-state geometry. The energy difference E is given in eV with respect to the ground state.

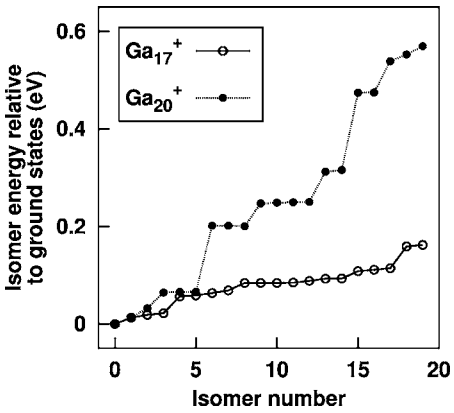

FIG. 3. The energies of the isomeric structures of Ga_{17}^+ and Ga_{20}^+ with respect to their ground states.

the top pentagon and the upper capped atom rearrange to accommodate the 20th atom, leading to a dome shaped hexagonal ring.

We now analyze the structural properties in detail to get an insight into the features that influence the melting characteristics. An analysis of the distribution of bond lengths shows that there are 12 bonds, in each cluster, with distances less than 2.55 Å.[28] However, for Ga_{17}^+, these short bonds are spread all over the cluster, whereas for Ga_{20}^+ they form the upper and the lower hexagonal rings. The distribution of coordination numbers[29] indicates that for Ga_{20}^+ almost all the atoms in the rings (about 16), have a coordination number of 4. The Ga_{17}^+ cluster does not have such a uniform distribution of coordination numbers. In this sense, Ga_{20}^+ is more ordered and symmetric than Ga_{17}^+.

Striking differences are also observed in the low energy isomers and their energy distribution. We obtained more than 200 distinct isomers spanning an energy range of about 2.5 eV above the ground state for each cluster. In Fig. 3 we plot the energies of first 20 isomers relative to the ground state. The isomers for the Ga_{17}^+ cluster appear to exhibit an almost continuous energy distribution. While a few of these isomers are severe distortions of the ground state geometry, the rest do not show any resemblance to the ground state [see Fig. 2(a)]. It appears that for Ga_{17}^+ in this low energy regime, small rearrangements of the atoms, costing just a small amount of energy, lead to several close-lying isomers, so that the isomer distribution is almost continuous. In contrast, the isomers of Ga_{20}^+ cluster are distributed in three groups separated by an energy gap of about 0.2 eV (Fig. 3). The first group of isomers have slightly different orientations of atoms in the hexagonal rings and are nearly degenerate with the ground state. The second group consists of structures having only the lower hexagonal ring while the third group has no rings. This indicates that the hexagonal units of Ga_{20}^+ cluster are stable and difficult to break up. The stability of the ring pattern of Ga_{20}^+ and the isomer distribution for both the clusters should have a substantial effect on the melting characteristics. Indeed, as we shall see further below these features play a crucial role in the finite temperature characteristics. It should be mentioned that although these observations are based on a limited search, we believe that the general features described here are essentially correct.

TABLE I. The number of basins with more than one atom at different values of the electron localization function (ELF) for the ground-state structures of Ga_{17}^+ and Ga_{20}^+ clusters. The numbers in parenthesis represent the number of atoms in each basin.

ELF value	Ga_{17}^+	Ga_{20}^+
0.85	0	1 (2)
0.77	1 (2)	2 (5,7)
0.75	3 (2,2,2)	2 (5,7)
0.73	2 (3,4)	1 (14)

The most important difference between the two clusters is in the nature of their bonding. We use the concept of electron localization function[30] (ELF) to describe the nature of bonding. The ELF is defined as

$$\eta(r) = \frac{1}{1 + \left(\frac{D_p}{D_h}\right)^2}, \tag{1}$$

$$D_h = \left(\frac{3}{10}\right)(3\pi^2)^{5/3}\rho^{5/3}, \tag{2}$$

$$D_p = \frac{1}{2}\sum_{i=1}^{N} |\nabla \psi_i|^2 - \frac{1}{8}\frac{|\nabla \rho|^2}{\rho}, \tag{3}$$

$$\rho = \sum_{i=1}^{N} |\psi_i(r)|^2. \tag{4}$$

Here $\rho(r)$ is the valance charge density. D_p is the excess local kinetic energy density due to Pauli repulsion and D_h is the Thomas-Fermi kinetic energy density. The numerical values of $\eta(r)$ are conveniently normalized to a value between zero and unity. A value of 1 represents a perfect localization of the valance charge while the value for the uniform electron gas is 1/2. Typically, the existence of an isosurface in the bonding region between two atoms at a high ELF value say, $\geqslant 0.70$, signifies a localized bond in that region.

Recently, Silvi and Savin[31] introduced a nomenclature for the topological connectivity of the ELF. According to this description, the molecular space is partitioned into regions or basins of localized electron pairs or attractors. At very low values of the ELF all the basins are connected. In other words, there is a single basin containing all the atoms. As the value of the ELF is increased, the basins begin to split and finally, we will have as many basins as the number of atoms. The value of the ELF at which the basins split is a measure of the interaction between the different basins (in chemical terms a measure the electron delocalization).

We have analyzed the electron localization functions for Ga_{17}^+ and Ga_{20}^+ clusters for values $\leqslant 0.85$. In Table I, we give the number of basins containing two or more atoms, for selected ELF values. The basins for Ga_{17}^+ show a fragmented growth pattern, each one containing very few atoms compared to Ga_{20}^+. For instance, at an isovalue of 0.75, while Ga_{17}^+ has three basins each having 2 atoms, Ga_{20}^+ has

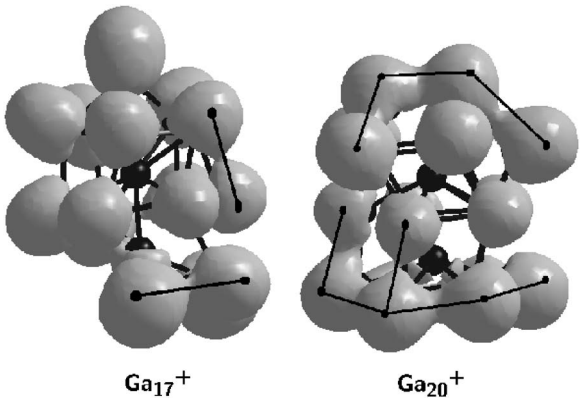

FIG. 4. The isosurface for the electron localization functions for Ga_{17}^+ and Ga_{20}^+ at an isovalue of 0.75. The black lines correspond to merged basin structures.

just two basins each containing 5 and 7 atoms, corresponding to the two hexagonal rings. The ELF contours for the isovalue of 0.75 are shown in Fig. 4. The merged basins structures are shown by the black lines. It may be inferred that the bonds between atoms in the hexagonal rings of Ga_{20}^+ are strong and covalent in nature with similar strengths, while the fragmented basin growth pattern in Ga_{17}^+ indicates inhomogeneity of the bond strengths.

The calculated, normalized, canonical specific heats are plotted against temperature in Fig. 5. The plot for Ga_{17}^+ exhibits a broad feature (apparently consisting of three components) which extends from 300 to 1400 K. For Ga_{20}^+, the calculated specific heat remains nearly flat up to about 600 K, it then increases sharply and peaks at about 800 K, in excellent agreement with the experimental results described above. Thus, the interesting size sensitive features seen in the experimental specific heats are reproduced in the simulations. The differences between Ga_{17}^+ and Ga_{20}^+ can be understood from our earlier discussion of the bondlength distributions, coordination numbers, isomer distributions, and the nature of bonding in these clusters. While the Ga_{17}^+ cluster shows no real evidence for ordered behavior, the Ga_{20}^+ cluster has well ordered ring patterns.

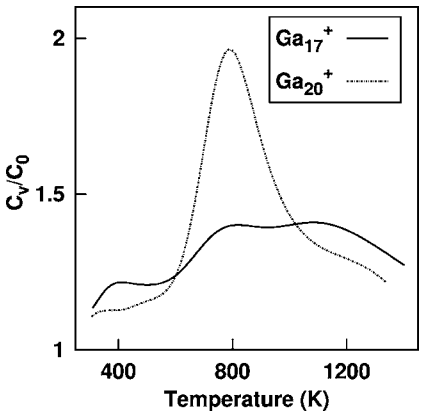

FIG. 5. Normalized canonical specific heat for Ga_{17}^+ (continuous line) and Ga_{20}^+ (dashed line). $C_0=(3n-6+3/2)k_B$ is the classical limit for the rotational plus vibrational canonical specific heat.

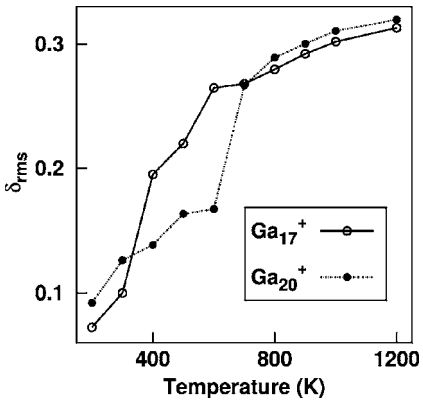

FIG. 6. Root mean square bond length fluctuations ($\delta_{\rm rms}$) for Ga_{17}^+ (continuous line) and Ga_{20} (dashed line).

Thus, when Ga_{17}^+ is heated, the bonds soften gradually, and the atoms within the cluster rearrange, reorient, or diffuse depending upon their kinetic energy. We have studied the motion of the ionic cores by visually examining the trajectories.[32] The trajectories for the Ga_{17}^+ cluster clearly show that this cluster smoothly evolves through its higher energy isomers as the temperature rises from 300 to 1400 K.

On the other hand, the ionic motion for Ga_{20}^+ shows only minor rearrangements of the atoms until 600 K, and then the cluster visits all the isomers corresponding to the first group of isomers described above. At about 700 K, the upper hexagonal ring breaks, while at about 800 K, the lower ring breaks. Thus, melting of Ga_{20}^+ cluster is associated with the breaking of the well ordered covalently bonded hexagonal units.

We have also analyzed the melting characteristics via traditional parameters such as the root mean squared bond length fluctuations ($\delta_{\rm rms}$) and the mean squared ionic displacements (MSD).[20,33] $\delta_{\rm rms}$ is defined as

$$\delta_{\rm rms} = \frac{2}{N(N-1)} \sum_{i<j} \frac{\sqrt{\langle R_{ij}^2 \rangle_t - \langle R_{ij} \rangle_t^2}}{\langle R_{ij} \rangle_t}, \tag{5}$$

where N is the number of particles in the system, R_{ij} is the distance between the ith and jth particles in the system, and $\langle \cdots \rangle_t$ denotes a time average over the entire trajectory. In Fig. 6, we show the $\delta_{\rm rms}$ for Ga_{17}^+ and Ga_{20}^+ clusters. This plot correlates well with the specific heat curve shown in Fig. 5. The $\delta_{\rm rms}$ for Ga_{17}^+ rises gradually from 300 K while for Ga_{20}^+ it rises sharply at about 700 K, and finally saturates at the same value for both the clusters. It may be inferred from this observation that the behavior of both the clusters at high temperatures, say $T \geqslant 800$ K, are similar and that both of them can be considered to be in liquidlike states. This conclusion is further substantiated by the MSD plots (figures not shown), which saturate at ≈ 21 Å^2 at about 1200 K. Thus the theoretical results support the interpretation that the inflection in the cross sections for Ga_{17}^+ results from a melting transition.

IV. SUMMARY AND CONCLUSION

It is evident from the present study that the nature of the ground-state geometry and the bonding between the atoms

strongly influences the finite temperature characteristics of Ga_{17}^+ and Ga_{20}^+. Ga_{20}^+ shows partial ordering in the sense of having well-defined units or rings. The atoms in these rings move together and the rings remain intact until 600 K. The melting of this cluster is associated with the disruption of the rings. The Ga_{17}^+, on the other hand, shows a distribution of bond energies, angles, and coordination numbers and a more continuous distribution of excited states. Melting here is a more gradual process, as the cluster evolves through the accessible isomers. At high temperatures, $T \geqslant 800$ K, both Ga_{17}^+ and Ga_{20}^+ have similar root mean squared bond length fluctuations and mean squared ionic displacements, so both of them can be considered to be in liquidlike states. The experimental results show that while Ga_{17}^+ apparently undergoes a solid-liquid transition without a significant peak in the specific heat, Ga_{20}^+ melts with a relatively sharp peak. The simulations reproduce this behavior, and show that if a cluster is "ordered" (i.e., a large fraction of the constituent atoms show similar bonding, coordination numbers, and bond energies) then it is likely to show a sharp melting transition with a significant peak in the specific heat.

These observations have interesting consequences for the finite temperature behavior of small clusters as a function of cluster size. It is likely that as the clusters grow in size, their structures evolve from one well ordered structure to another, passing on the way through some cluster sizes that have "disordered" structures. For instance, the 13 atom gallium cluster is predicted to have a highly symmetric decahedron structure with a bonding pattern that is similar to that found here for Ga_{20}^+.[12] So in the present case, cluster growth from Ga_{13} (a decahedron) to (Ga_{20}^+, a distorted double decahedron) proceeds via a disordered Ga_{17}^+ structure. Such a behavior is also observed for sodium clusters of 40 to 55 atoms; the ground-state geometries of Na_{40} and Na_{55} are either icosahedral or close to icosahedral while that of Na_{50} has no particular symmetry.[17,18] In such cases, we expect that the specific heats should change from showing a well defined peak to a rather broad one, and back again to well defined. We believe this behavior to be generic as it has not only been observed in the case of gallium clusters[8,9] but also in case of aluminum clusters[10] experimentally, and for sodium clusters in the simulations mentioned above.

ACKNOWLEDGMENTS

The financial support of the Indo French Center for Promotion of Advanced Research is gratefully acknowledged. C-DAC (Pune) is acknowledged for providing us with the supercomputing facilities. We gratefully acknowledge partial support of this work by the U.S. National Science Foundation.

[1] P. Pawlow, Z. Phys. Chem., Stoechiom. Verwandtschaftsl. **65**, 545 (1909).
[2] P. R. Couchman and W. A. Jesser, Nature (London) **269**, 481 (1977).
[3] M. Schmidt, R. Kusche, W. Kronmüller, B. von Issendorff, and H. Haberland, Phys. Rev. Lett. **79**, 99 (1997).
[4] M. Schmidt, R. Kusche, B. von Issendorf, and H. Haberland, Nature (London) **393**, 238 (1998).
[5] M. Schmidt, J. Donges, Th. Hippler, and H. Haberland, Phys. Rev. Lett. **90**, 103401 (2003).
[6] H. Haberland, T. Hippler, J. Donges, O. Kostko, M. Schmidt, and B. von Issendorff, Phys. Rev. Lett. **94**, 035701 (2005).
[7] A. A. Shvartsburg and M. F. Jarrold, Phys. Rev. Lett. **85**, 2530 (2000).
[8] G. A. Breaux, R. C. Benirschke, T. Sugai, B. S. Kinnear, and M. F. Jarrold, Phys. Rev. Lett. **91**, 215508 (2003).
[9] G. A. Breaux, D. A. Hillman, C. M. Neal, R. C. Benirschke, and M. F. Jarrold, J. Am. Chem. Soc. **126**, 8682 (2004).
[10] G. A. Breaux, C. M. Neal, B. Cao, and M. F. Jarrold, Phys. Rev. Lett. **94**, 173401 (2005).
[11] G. A. Breaux, C. M. Neal, B. Cao, and M. F. Jarrold, Phys. Rev. B **71**, 073410 (2005).
[12] S. Chacko, Kavita Joshi, and D. G. Kanhere, Phys. Rev. Lett. **92**, 135506 (2004).
[13] K. Joshi, D. G. Kanhere, and S. A. Blundell, Phys. Rev. B **66**, 155329 (2002).
[14] K. Joshi, D. G. Kanhere, and S. A. Blundell, Phys. Rev. B **67**, 235413 (2003).
[15] F.-C. Chuang, C. Z. Wang, S. Ogut, J. R. Chelikowsky, and K. M. Ho, Phys. Rev. B **69**, 165408 (2004).
[16] K. Manninen, A. Rytkönen, and M. Manninen, Eur. J. Phys. **29**, 39 (2004).
[17] S. Chacko, D. G. Kanhere, and S. A. Blundell, Phys. Rev. B **71**, 155407 (2005).
[18] Mal-Soon Lee, S. Chacko, and D. G. Kanhere, J. Chem. Phys. (to be published).
[19] A. M. Ferrenberg and R. H. Swendsen, Phys. Rev. Lett. **61**, 2635 (1988); P. Labastie and R. L. Whetten, *ibid.* **65**, 1567 (1990).
[20] D. G. Kanhere, A. Vichare, and S. A. Blundell, *Reviews in Modern Quantum Chemistry*, edited by K. D. Sen (World Scientific, Singapore, 2001).
[21] E. A. Mason and E. W. McDaniel, *Transport Properties of Ions in Gases* (Wiley, New York, 1988).
[22] D. E. Clemmer and M. F. Jarrold, J. Mass Spectrom. **32**, 577 (1997).
[23] M. C. Payne, M. P. Teter, D. C. Allen, T. A. Arias, and J. D. Joannopoulos, Rev. Mod. Phys. **64**, 1045 (1992).
[24] D. Vanderbilt, Phys. Rev. B **41**, R7892 (1990).
[25] Vienna *ab initio* simulation package, Technische Universität Wien, 1999; G. Kresse and J. Furthmüller, Phys. Rev. B **54**, 11169 (1996).
[26] In our earlier work on gallium clusters (see Ref. 12), we have verified that the *d* electrons do not significantly affect the equilibrium geometries and the finite temperature behavior.
[27] A. Vichare, D. G. Kanhere, and S. A. Blundell, Phys. Rev. B **64**, 045408 (2001).
[28] A typical bond distance of a metallic bond seen in the extended system, i.e., α gallium, is about 2.79 Å.

[29] The coordination number is computed by counting the number of atom lying within a sphere of radius of 2.79 Å. The radius 2.79 Å is chosen since this value corresponds to the maximum bond length of a metallic bond in the α Ga bulk phase. For a description of α Ga see, for instance, X. G. Gong, G. L. Chiarotti, M. Parrinello, and E. Tosatti, Phys. Rev. B **43**, 14277 (1991); V. Heine, J. Phys. C **1**, 222 (1968); V. Heine and D. Weaire, Solid State Phys. **24**, 249 (1970).

[30] A. D. Becke and K. E. Edgecombe, J. Chem. Phys. **92**, 5397 (1990).

[31] B. Silvi and A. Savin, Nature (London) **371**, 683 (1994).

[32] A package for displaying MOLecular DENsity, written by G. Schaftenaar, CAOS/CAMM Center Nijmegen, Toernooiveld, Nijmegen, The Netherlands, was employed.

[33] R. S. Berry and H. Haberland, *Clusters of Atoms and Molecules I*, edited by H. Haberland (Springer-Verlag, Berlin, 1994).